3 (2026) 100026

Contents lists available at ScienceDirect

Journal of Hazardous Materials: Organics

journal homepage: www.sciencedirect.com/journal/journal-of-hazardous-materials-organics

Exploring the synergistic sorption capacities of magnetic-chitosan-*Arthrospira platensis* biocomposite for simultaneous removal of tetracycline and heavy metals

Shabnam Mirizadeh *, Alessandro Alberto Casazza, Attilio Converti

Department of Civil, Chemical, and Environmental Engineering, Genoa University, Pole of Chemical Engineering, via Opera Pia 15, Genoa I-16145, Italy

ARTICLE INFO

Keywords:
Tetracycline
Heavy metals
Co-adsorption
Magnetic biocomposite

ABSTRACT

The frequent co-occurrence of antibiotics and heavy metals in aquatic environments significantly affects their adsorption properties and removal efficiency. This study investigated the co-adsorption behavior of tetracycline (TC) and heavy metals (Pb, Cr, and Ni) using a magnetic chitosan/*A. platensis* (MCA) biocomposite as a biosorbent. Experiments were conducted on both single and binary systems to compare the biocomposite's efficiency in adsorbing these pollutants. Results revealed that lead (Pb) enhanced TC adsorption through a synergistic effect, whereas chromium (Cr) and nickel (Ni) exhibited competitive interactions, reducing TC removal. TC removal reached 54% in the single system but increased to as much as 91.2% in the presence of 10 mg/L Pb. Adsorption equilibrium data were well described by the Langmuir model, implying monolayer coverage. The highest adsorption capacities were 505.91 and 421.40 mg/g for TC, and 518.39 and 495.26 mg/g for Pb in the binary and single systems, respectively. Kinetic experiments demonstrated that adsorption conformed to a pseudo-second-order model, suggesting chemisorption as the rate-controlling step, while thermodynamic parameters confirmed that the process was endothermic and spontaneous. These outcomes suggest that the MCA biocomposite is a promising solution for removing antibiotics and heavy metals from contaminated water.

1. Introduction

In recent decades, the extensive use of antibiotics and the discharge of heavy metals from industrial activities have become one of the major environmental concerns. These types of pollutants are known to be non-biodegradable and highly toxic to both human health and wildlife [1,2]. Their harmful effects can become more pronounced when they coexist in complex mixtures, as their different chemical and physical characteristics can lead to synergistic or antagonistic interactions [3,4].

Tetracycline (TC) is one of the broad-spectrum antibiotics that has often been cited as an example of a pharmaceutical pollutant. Due to its effectiveness and low cost, it is widely used in veterinary medicine [5,6]. However, TC is known not to be completely metabolized under physiological conditions [7]; therefore, it has been detected in surface water, groundwater, and even drinking water [6,8]. As a result, long-term exposure to TC may lead to adverse health effects, such as liver damage and growth abnormalities [9].

Similarly, heavy metals such as lead (Pb), chromium (Cr), and nickel (Ni) are also ubiquitous pollutants, originating from numerous sources such as industrial processes, urban runoff, and the natural environment [10]. Pb, a byproduct of mining, smelting, and battery manufacturing, is highly toxic even in trace amounts and bioaccumulates in aquatic ecosystems, causing significant harm to organisms and human health [11]. Cr, especially in its hexavalent form, is dangerous, as it is a confirmed carcinogen and can be harmful if ingested, inhaled, or if it comes into contact with the skin [12]. Ni is commonly used in electroplating and steelmaking, contaminating water bodies and causing skin allergy, respiratory problems, and other health issues. These metals are also found in nature at very low concentrations, but their levels have increased due to human activities and, consequently, have adversely affected environmental and human health [13].

Various remediation techniques, such as chemical precipitation, ion exchange, membrane filtration, photocatalysis, adsorption, and electrochemical methods, have been employed to remove antibiotics and heavy metals from contaminated environments [14–18]. Among them, adsorption has attracted great interest due to its cost-effectiveness,

* Corresponding author.
E-mail address: shabnam.mirizadeh@edu.unige.it (S. Mirizadeh).

https://doi.org/10.1016/j.hazmo.2026.100026
Received 4 February 2026; Received in revised form 13 April 2026; Accepted 13 April 2026
Available online 15 April 2026

operational simplicity, and flexibility. A wide range of adsorbents, such as activated carbon, clays, biochar, and biopolymers, have been investigated to evaluate their effectiveness in removing these contaminants [19,20]. Natural polymers, particularly chitosan [21], have emerged as promising adsorbents for removing various contaminants due to their biodegradability, low cost, and availability. Being a chitin-derived biopolymer, chitosan possesses functional groups (hydroxyl and amine groups) capable of establishing strong interactions with both organic and inorganic pollutants. However, its potential applications are limited by unsatisfactory mechanical properties and difficult post-removal recovery [22–24].

To overcome such restraints, chitosan-based composites with enhanced surface area, mechanical strength, and adsorption performance have been explored [25–28]. *Arthrospira platensis,* a nutrient-rich cyanobacterium, is well known to be used in biosorption because it contains high levels of polysaccharides and proteins that provide active binding sites to pollutants [29–31]. Incorporating chitosan into *A. platensis* biomass in the form of magnetic composite materials can improve adsorption performance, as well as mechanical stability and reusability. In a previous study, a magnetic chitosan-*A. platensis* (MCA) composite showed a very high TC adsorption capacity (approximately 830 mg/g) [32].

Despite advances in adsorption technology, most reported studies have only examined the removal of organic or inorganic pollutants individually. Therefore, research on the concurrent removal of antibiotics and heavy metals in binary systems is relatively scarce and limited [33,34], resulting in a considerable gap in the understanding of their interactions in the adsorption process [35,36]. It is therefore necessary to fill this gap to develop versatile adsorbents capable of handling complex pollutant mixtures.

According to previous findings, the current study investigates the adsorption performance of the same MCA composite in a co-adsorption process involving TC in combination with Pb, Cr, and Ni. The goal is to provide insights into the development of sustainable, high-performance adsorbents capable of concurrently combating existing antibiotic and heavy metal contamination, thereby enhancing environmental remediation strategies.

2. Materials and methods

2.1. Batch adsorption experiments

TC and heavy metals (Pb, Cr, and Ni) removal was evaluated through batch experiments using the MCA biocomposite, which was prepared and characterized by Mirizadeh et al. [32]. In this regard, freshly prepared stock solutions and deionized water were used in all tests to ensure consistency. Such an adsorbent was added at a dosage of 0.1 g/L to pollutant solutions, which were agitated at 120 rpm using a shaker operating at a temperature of 23 ± 2 °C. The solution pH was maintained between 5.5 and 6.0 to prevent the formation of metal hydroxides. Experiments were conducted in two distinct modes: single-component systems and binary systems containing both TC and heavy metals. Fig. 1 provides a graphical representation of the experimental procedure.

Kinetic studies on TC adsorption were conducted at initial metal ion concentrations of 5 and 10 mg/L. Additionally, experiments were performed with 10 mg/L of heavy metals in the presence of TC concentrations of 10 and 25 mg/L. Isotherm studies were carried out at initial concentrations ranging from 1 to 100 mg/L for metal ions and 10–150 mg/L for TC. For the thermodynamic study, adsorption was evaluated at three different temperatures (298, 308, and 318 K) under pre-optimized conditions, and the main thermodynamic parameters were estimated.

The concentrations of metal ions before and after adsorption were measured using an atomic absorption spectrometer (AA240FS, Varian, Milan, Italy) equipped with a Vapor Generation Accessory (VGA-77, Varian). TC concentrations were determined by UV–Vis spectrophotometry at a wavelength of 360 nm. All experiments were conducted in duplicate, and the average values were reported.

The removal percentage (Y, %), adsorption capacity at a given time t (q_t, mg/g), and equilibrium adsorption capacity (q_e, mg/g) were calculated according to the following equations:

$$Y(\%) = \left(\frac{C_0 - C_e}{C_0}\right) \times 100 \quad (1)$$

$$q_t = \frac{(C_0 - C_t)V}{m} \quad (2)$$

$$q_e = \frac{(C_0 - C_e)V}{m} \quad (3)$$

where C_0, C_t, and C_e (mg/L) are the initial, residual, and equilibrium concentrations, respectively, m is the mass of dried adsorbent (g), and V refers to the solution volume (L).

2.2. Isotherm, kinetic, and thermodynamic of the adsorption process

Adsorption isotherms were examined using Langmuir, Freundlich, Temkin, and Dubinin-Radushkevich (D-R) models to interpret the adsorption behavior. The Langmuir model, which assumes monolayer adsorption formation and uniform adsorption energy, is represented as follows:

$$q_e = \frac{K_L q_m C_e}{1 + K_L C_e} \quad (4)$$

where q_m (mg/g) represents the theoretical maximum capacity for monolayer coverage, while K_L (L/mg) is the Langmuir constant that indicates the interaction strength between adsorbate molecules and

Fig. 1. Graphical representation of the experiment procedure.

available adsorption sites.

The Freundlich isotherm explains adsorption occurring on surfaces that are uneven or heterogeneous:

$$q_e = K_F C_e^n \quad (5)$$

where K_F ((mg/g) (L/mg) $^{-1/n}$) is the Freundlich constant, and n represents the heterogeneity factor.

The Temkin model describes a gradual reduction in adsorption heat as surface coverage increases:

$$q_e = \frac{RT}{b_T} \ln (A_T C_e) \quad (6)$$

where A_T (L/mg) represents the equilibrium association constant, and b_T (J/mol) is a factor related to the adsorption energy.

The D-R model considers the pore size and distribution of the adsorbent:

$$q_e = q_s \exp(-B\varepsilon^2) \quad (7)$$

where q_s (mg/g) denotes the theoretical saturation capacity, B (mol^2/kJ^2) is a constant factor related to the average adsorption energy (E) (kJ/mol), and ε (kJ/mol) represents the Polanyi potential energy. The formulas for ε and E are given below:

$$\varepsilon = RT \ln(1+\frac{1}{C_e}) \quad (8)$$

$$E = \frac{1}{\sqrt{2B}} \quad (9)$$

The pseudo-first-order (PFO) (Eq. 10) and pseudo-second-order (PSO) (Eq. 11) models were employed to examine adsorption kinetics:

$$\ln (q_e - q_t) = \ln q_e - k_1 t \quad (10)$$

$$\frac{t}{q_t} = \frac{1}{k_2 q_e^2} + \frac{1}{q_e} t \quad (11)$$

where k_1 (1/min) and k_2 (g/mg·min) are the rate constants for the PFO and PSO models, respectively.

Thermodynamic studies were carried out under optimized conditions to assess key parameters, including the standard Gibbs free energy (ΔG°, kJ/mol), enthalpy (ΔH°, kJ/mol), and entropy (ΔS°, J/mol.K) changes, which were calculated as follows:

$$\Delta G^\circ = -RT \ln K_D \quad (12)$$

$$\Delta G^\circ = \Delta H^\circ - T\Delta S^\circ \quad (13)$$

where K_D (q_e/C_e) is the distribution coefficient.

3. Results and discussion

3.1. Adsorption and co-adsorption of tetracycline and heavy metals

In the first part of this study, TC adsorption at a starting concentration of 50 mg/L and its co-adsorption with Pb, Cr, and Ni at initial concentrations of 5, 10, and 20 mg/L were assessed. The experiments were performed over time, as depicted in Fig. 2.

The efficiency of TC adsorption, examined in terms of Ct/C_o ratio, was shown to be greatly affected by the presence and concentrations of heavy metals. In the absence of heavy metals, the MCA biocomposite allowed for a TC removal of 54.03%, which corresponded to a Ct/C_o reduction up to 0.46 in 180 min. Interestingly, the addition of Pb at initial concentrations of 5 and 10 mg/L enhanced TC adsorption, indicating a synergistic effect. This improvement in adsorption efficiency can be attributed to the ability of Pb ions to strengthen the binding forces between TC and the biocomposite [37]. Nevertheless, at 20 mg/L Pb, the synergistic effect decreased, most likely owing to the saturation of active binding sites on the biocomposite.

On the contrary, Cr competed with TC for the adsorption sites. The Ct/C_o ratio observed in the presence of 5 mg/L Cr (0.517), was moderately higher than that of the control (TC only), pointing to a reduction in the efficiency of TC adsorption. With the increase in Cr concentration to 10 and 20 mg/L, the adsorption efficiency continued to decline, which suggests that Cr ions were occupying the adsorption sites available for TC.

Ni also showed a nearly identical effect. At its lowest concentration (5 mg/L), it led to a slight increase in TC adsorption. However, as the concentration of Ni increased to 10 and 20 mg/L, higher Ct/C_o ratios were observed, indicating a significant reduction in TC removal efficiency. This could be explained by the competitive effect of Ni at higher concentrations, which reduces the availability of active binding sites for TC.

The different effects of heavy metals on TC adsorption can be attributed to the distinct chemical interactions among each metal ion, the adsorbent, and the TC molecules [38]. Pb evidently had a greater affinity for the various functional groups, such as amino (-NH₂), hydroxyl (-OH), and carboxyl (-COOH) groups, present on the surface of the biocomposite.

This strong interaction may have been responsible for the stabilization of Pb-TC complexes via coordination bonds or electrostatic interactions. Such complexes may have improved TC adsorption by increasing the overall affinity for the biocomposite surface. In particular, the Pb ion can act as a bridge between TC and the adsorbent, which allows it to stabilize the attachment of TC and facilitates multilayer adsorption or co-adsorption mechanisms [37,39–41]. For example,

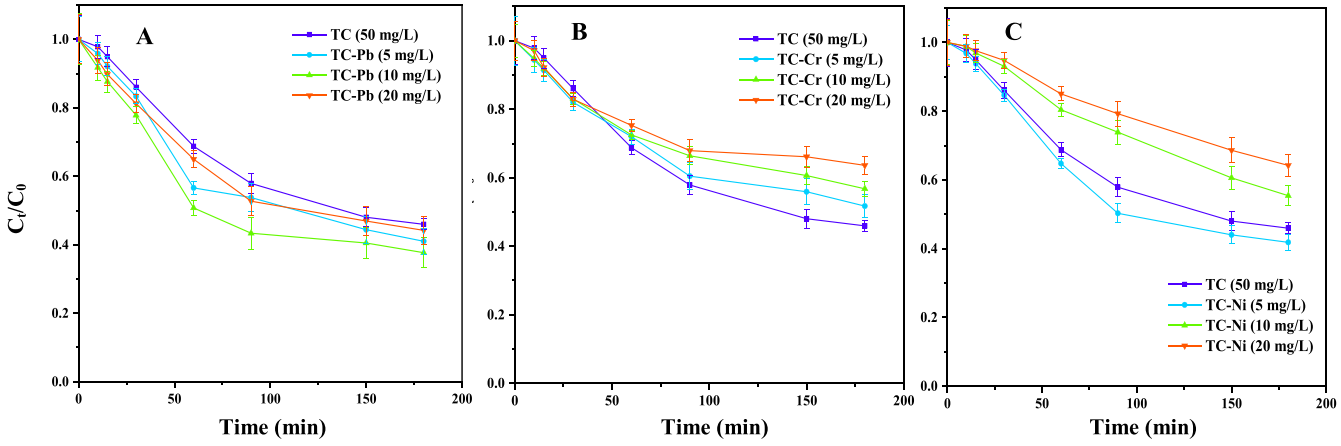

Fig. 2. Removal of TC over time, either alone or in the presence of Pb (A), Cr (B), and Ni (C) at different initial concentrations (5, 10, and 20 mg/L).

Zheng et al. reported an increased TC adsorption in the presence of Cu via a bridging effect on magnetic chitosan biosorbent [42].

Conversely, Cr and Ni directly competed with TC for the same adsorption sites. These metal ions can exert strong electrostatic attractions on negatively charged functional groups, thus limiting the number of sites available for binding to TC molecules [43]. With the increase in metal concentration, the competition for adsorption at the active sites of the biocomposite has likely become more significant. Besides, Cr and Ni may not readily form complexes with TC or may form weaker interactions compared to Pb, further enhancing the competition.

The removal of heavy metals (Pb, Cr, and Ni) at an initial concentration of 10 mg/L was also influenced by the presence of TC at initial concentrations of 10, 25, and 50 mg/L (Fig. 3).

Pb showed the highest removal efficiency of 91.20% at 10 mg/L TC. However, at 25 and 50 mg/L TC, Pb removal efficiency decreased to 79.16 and 68.93%, respectively, likely due to higher competition for adsorption sites.

Cr and Ni removal efficiencies were lower than that of Pb. Particularly, Cr showed removal efficiencies of 68.50, 69.10, 61.01, and 58.41% in the presence of TC at concentrations of 0, 10, 25, and 50 mg/L, respectively. Ni also followed the same trend, with removal efficiencies of 68.51, 65.08, 60.90, and 56.14% under the same conditions.

The adsorption efficiency of the biocomposite towards Cr and Ni consistently decreased with increasing TC concentration, confirming that both metals are more subject to competitive inhibition by TC [38,44].

These findings highlight that Pb has the highest adsorption affinity among the heavy metals tested, possibly due to its chemical properties, including a larger ionic radius, higher charge density, and stronger electrostatic interactions with the biocomposite [45,46].

3.2. Kinetics, isotherms, and thermodynamic study

The kinetics of TC adsorption in the presence of Pb, Cr, and Ni at concentrations of 5 and 10 mg/L were analyzed by PFO and PSO models (Fig. 4), and the results of the respective kinetic parameters are listed in Table 1.

The experimental values of the equilibrium adsorption capacities ($q_{e,exp}$) indicated clear differences in adsorption behavior depending on the type and concentration of heavy metals. The PSO model best predicted the trial data with a higher range of determination coefficient (R^2 of 0.960–0.996) compared to that of the PFO model (0.865–0.979). This confirms that the major mechanism was chemisorption in TC adsorption in all the systems [47]. The equilibrium adsorption capacity values predicted using the PSO model were in good agreement with the experimental ones, especially for the TC-Ni and TC-Cr systems. Similarly, the adsorption kinetics of Pb, Cr, and Ni in the presence of TC at the concentrations of 10 and 25 mg/L were also evaluated (Fig. 5).

The PSO model consistently provided a closer correlation to experimental data, evidenced by much higher R^2 values (0.977–0.996) compared to the PFO model (0.850–0.953). The values of equilibrium adsorption capacity predicted by the PSO model also aligned better the experimental results, and the higher PSO rate constants reflected better adsorption kinetics, particularly for Cr and Ni at lower TC concentrations. These findings support the validity of the PSO model in describing the adsorption processes [47,48].

The isotherm study of TC and heavy metals removal was carried out by using four isotherm models, namely Langmuir, Freundlich, Dubinin-Radushkevich (D-R), and Temkin models. The fitting parameters of each model describing the adsorption behavior and mechanisms are presented in Table 2, while Figs. 6 and 7 show the Langmuir isotherm fits.

The Langmuir model closely described TC adsorption and its co-adsorption with heavy metals, and with R^2 values consistently above 0.98. The maximum TC adsorption capacity (q_{max}) increased up to 505.91 mg/L when Pb concentration was 10 mg/L, suggesting higher synergy in adsorption. However, using Cr and Ni at the same concentration, q_{max} decreased slightly to 387.79 and 383.97 mg/g, respectively, which is a sign of competitive adsorption. Although the Langmuir model provided the best overall fit, the Freundlich, Temkin, and D–R models also showed high R^2 values (> 0.90). This suggests that these models offer valuable additional insights into adsorption behavior, including favorability, affinity, adsorbate–adsorbent interactions, and adsorption energy, especially when competing metal ions are present.

The Freundlich model parameters revealed that TC adsorption in the presence of Pb occurred with higher K_F values and n values below 1 for all systems, which is evidence of favorable adsorption of the mixture of TC and heavy metals. In the presence of Cr and Ni, K_F values declined significantly at higher concentrations, indicating lower affinity due to competition between metal ions and TC. The D-R model allowed to estimate a TC adsorption energy ($E = 0.225$ kJ/mol) compatible with physisorption, as the dominant mechanism. The E value increased with the co-adsorption of Pb at a concentration of 10 mg/L, suggesting slight chemical bonding. Conversely, the presence of Cr and Ni at higher concentrations reduced E to less than 0.16 kJ/mol, suggesting weaker physisorption-mediated interactions. The Temkin isotherm model takes into consideration the adsorbate-adsorbent interaction effect. In TC-Pb systems, b_T increased at higher Pb concentrations, reaching 1.602 J/mol, indicating stronger binding energies. However, in TC-Ni systems at 10 mg/L, b_T declined significantly, suggesting less favorable adsorbate-adsorbent interactions.

The adsorption of Pb, Cr, and Ni was also compared in the presence of TC (Fig. 7). Pb demonstrated the maximum q_{max} value (518.389 mg/g

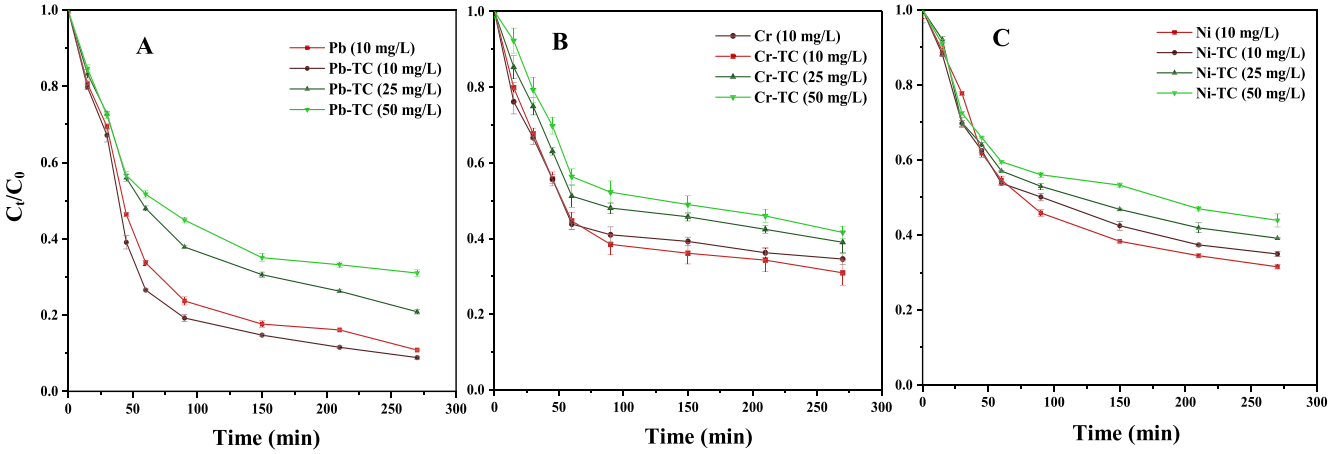

Fig. 3. Removal of Pb (A), Cr (B), and Ni (C) over time either alone or presence of TC at different initial concentrations (10, 25, and 50 mg/L).

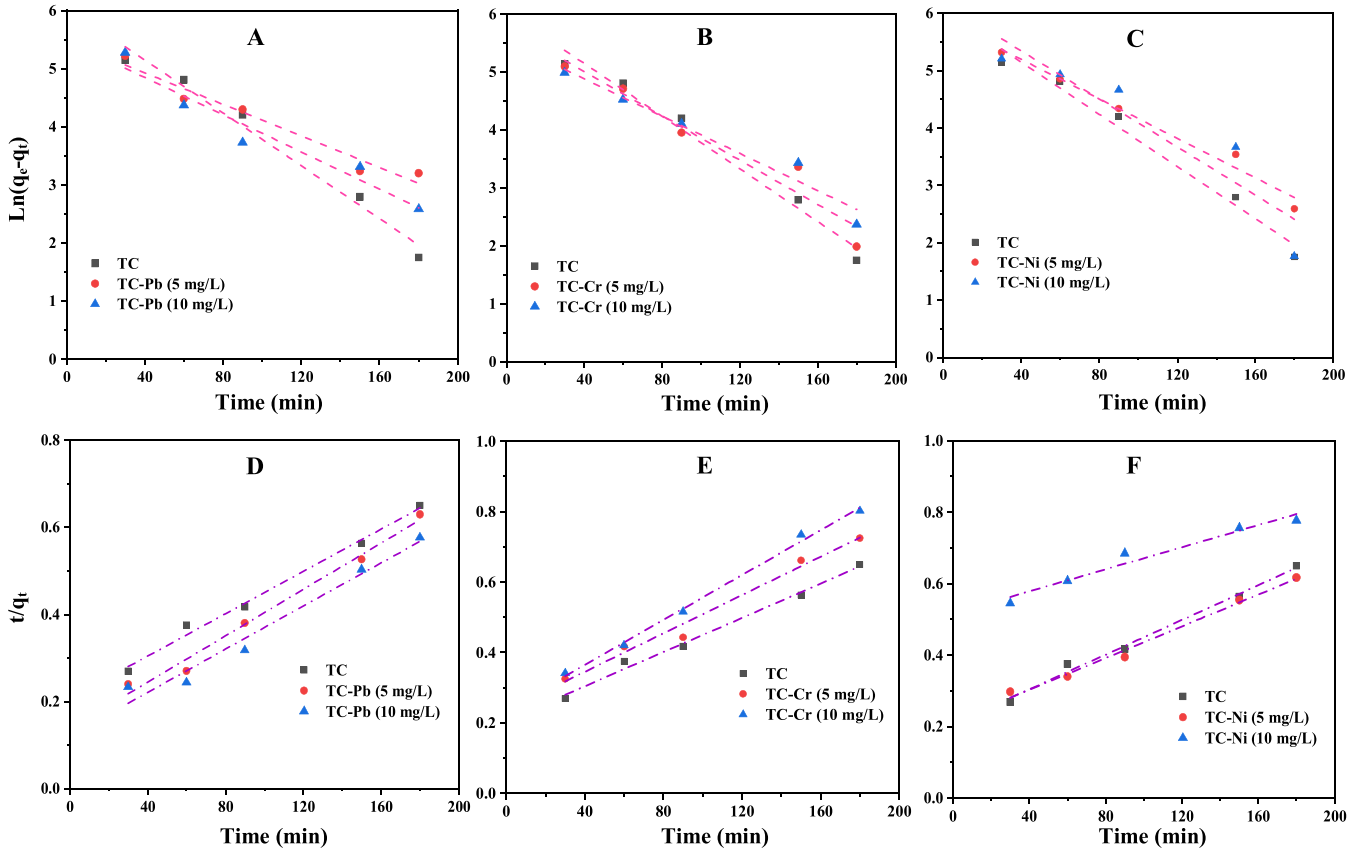

Fig. 4. Plots of kinetic PFO (A–C) and PSO (D–F) models, describing TC adsorption in the absence and the presence of Pb, Cr, and Ni at concentrations of 5 and 10 mg/L.

Table 1
Values of parameters and determination coefficients (R^2) from kinetic models used to investigate TC and heavy metals (Pb, Cr, and Ni) adsorption onto MCA biocomposite.

Adsorbent	PFO			PSO		
	$q_{e,cal}$	k_1	R^2	$q_{e,cal}$	$k_2 \times 10^3$	R^2
TC	428.375	0.023	0.979	411.523	0.029	0.992
TC-Pb (5 mg/L)	338.651	0.014	0.957	416.667	0.052	0.986
TC-Pb (10 mg/L)	341.530	0.016	0.940	403.226	0.051	0.969
TC-Cr (5 mg/L)	321.366	0.019	0.941	367.647	0.031	0.982
TC-Cr (10 mg/L)	351.117	0.016	0.959	313.480	0.043	0.996
TC-Ni (5 mg/L)	360.615	0.017	0.979	370.001	0.023	0.990
TC-Ni (10 mg/L)	384.724	0.021	0.865	312.501	0.323	0.960
Pb	74.630	0.012	0.953	119.047	0.167	0.996
Pb-TC (10 mg/L)	78.469	0.014	0.893	116.270	0.217	0.995
Pb-TC (25 mg/L)	81.126	0.012	0.933	112.360	0.123	0.995
Cr	67.530	0.011	0.870	101.012	0.156	0.976
Cr-TC (10 mg/L)	51.857	0.012	0.850	97.088	0.211	0.978
Cr-TC (25 mg/L)	56.872	0.009	0.870	84.746	0.210	0.978
Ni	104.168	0.132	0.911	104.168	0.132	0.990
Ni-TC (10 mg/L)	74.630	0.012	0.953	119.047	0.167	0.996

at 10 mg/L TC) according to the Langmuir isotherm. Conversely, the q_{max} values for Cr and Ni decreased with increasing TC concentration, highlighting competition for the adsorption sites. K_F values from the Freundlich model also showed similar trends, with Pb exhibiting the strongest multilayer adsorption affinity, while Cr and Ni reducing K_F as TC concentration increased. The values of E of the D-R model were less than 1 kJ/mol across all conditions, further confirming dominance of physisorption [49]. Temkin model b_T values were consistent with these findings, with Pb-TC systems possessing the strongest binding interactions.

The thermodynamic parameters, including the standard changes of Gibbs free energy (ΔG°), enthalpy (ΔH°) and entropy (ΔS°), were calculated to understand the nature of TC adsorption in the presence of heavy metals (Pb, Cr, Ni), and heavy metals adsorption in the presence of TC on MCA biocomposite. The values of ΔG° were determined at different temperatures (298 K, 308 K, and 318 K), while ΔH° and ΔS° were derived from Van't Hoff plots. The values of these thermodynamic parameters are given in Table 3.

All ΔG° values were negative across the studied temperatures, confirming the spontaneous nature of the adsorption process [50]. Moreover, ΔG° became more negative with increasing temperature, indicating that higher temperatures more favorable adsorption.

Among the metal ions, Pb showed the most negative ΔG° values (-10.97 to −12.84 kJ/mol), suggesting a stronger affinity of the biocomposite for Pb. Conversely, the TC-Ni system (10 mg/L) exhibited the least negative ΔG° values (-5.25 to −5.91 kJ/mol), indicating relatively weaker interactions. Positive ΔH° values for all systems suggest that the adsorption process is endothermic. The adsorption of TC alone took place with a ΔH° value of 18.21 kJ/mol, but this parameter was influenced by the presence of heavy metals. The enthalpy change. The highest ΔH° value (23.13 kJ/mol) was observed for the Ni-TC system (25 mg/L), implying stronger energy requirements for adsorption, possibly due to competition between TC and Ni for active sites [51].

All systems showed positive ΔS° values, indicating greater randomness at the interface between the adsorbent and solution. TC alone showed a ΔS° value of 81.83 J/mol·K, but this parameter increased in the presence of metals, achieving a maximum value of 102.84 J/mol·K in the Ni-TC system (25 mg/L) The increase in disorder likely resulted from the removal of water molecules and structural rearrangement of the adsorbate and adsorbent during adsorption [51].

The adsorption of Pb alone resulted in a high ΔS° value (93.47 J/

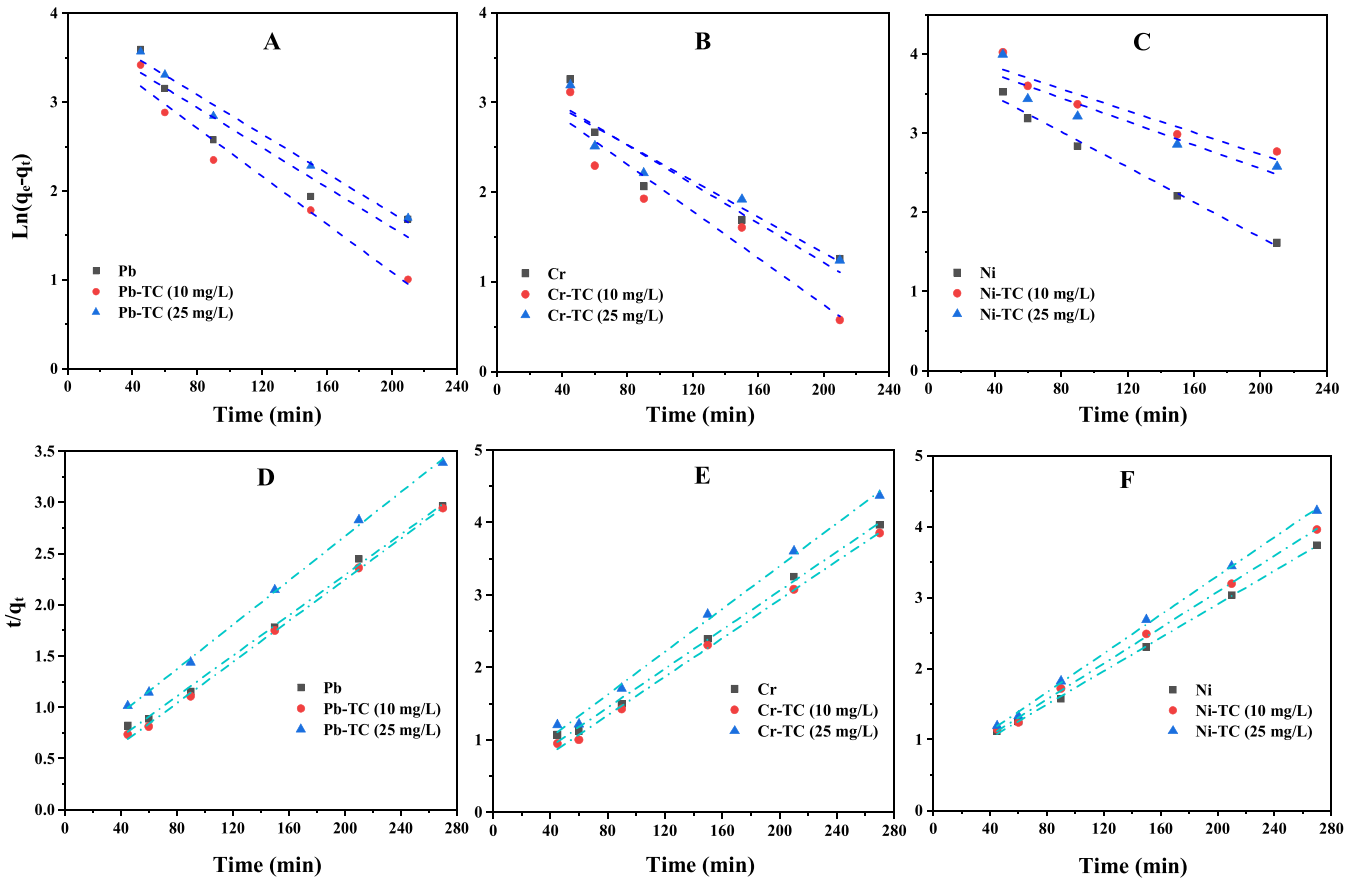

Fig. 5. Plots of kinetic PFO (A–C) and PSO (D–F) models, describing the adsorption of Pb, Cr, and Ni with and without TC at concentrations of 10 and 25 mg/L.

Table 2
Values of parameters and determination coefficients (R^2) from isotherm models used to investigate TC and heavy metals (Pb, Cr, and Ni) adsorption onto MCA biocomposite.

Adsorbent	Langmuir			Freundlich			D-R				Temkin		
	q_m	K_L	R^2	n	K_F	R^2	q_s	B	E	R^2	b_T	A_T	R^2
TC	421.399	0.086	0.993	0.320	90.380	0.923	360.734	9.917	0.225	0.916	30.850	1.179	0.974
TC-Pb (1 mg/L)	430.857	0.088	0.989	0.314	95.241	0.939	369.321	9.631	0.228	0.904	31.706	1.486	0.975
TC-Pb (5 mg/L)	469.363	0.093	0.985	0.315	105.160	0.909	402.740	8.778	0.239	0.924	28.368	1.404	0.960
TC-Pb (10 mg/L)	505.912	0.105	0.984	0.308	119.386	0.910	433.826	6.265	0.283	0.902	26.538	1.602	0.962
TC-Cr (1 mg/L)	429.973	0.084	0.992	0.323	90.749	0.932	365.721	9.976	0.224	0.908	30.587	1.218	0.976
TC-Cr (5 mg/L)	415.537	0.053	0.981	0.368	66.162	0.907	340.877	25.478	0.140	0.932	28.669	0.583	0.963
TC-Cr (10 mg/L)	387.790	0.046	0.984	0.385	54.992	0.914	313.420	29.775	0.130	0.934	29.910	0.469	0.970
TC-Ni (1 mg/L)	432.886	0.084	0.994	0.324	91.263	0.929	367.714	9.723	0.227	0.902	29.772	1.128	0.979
TC-Ni (5 mg/L)	442.735	0.090	0.990	0.316	97.565	0.917	381.199	9.746	0.227	0.923	29.052	1.178	0.968
TC-Ni (10 mg/L)	383.968	0.057	0.986	0.359	64.252	0.911	315.042	18.885	0.163	0.913	31.364	0.639	0.967
Pb	495.526	0.221	0.998	0.358	117.889	0.929	426.320	1.122	0.668	0.957	32.096	5.936	0.937
Pb-TC (10 mg/L)	518.389	0.226	0.999	0.367	121.623	0.939	448.816	1.255	0.631	0.950	29.541	5.353	0.959
Pb-TC (25 mg/L)	500.781	0.166	0.984	0.366	110.161	0.908	426.449	1.994	0.501	0.976	34.336	6.320	0.881
Pb-TC (50 mg/L)	500.775	0.118	0.986	0.407	88.752	0.894	412.390	3.281	0.391	0.960	32.133	4.279	0.846
Cr	530.791	0.088	0.976	0.451	76.405	0.926	411.743	4.828	0.322	0.981	33.556	3.653	0.852
Cr-TC (10 mg/L)	526.237	0.105	0.968	0.415	89.025	0.914	424.195	3.582	0.374	0.985	33.577	4.468	0.861
Cr-TC (25 mg/L)	523.881	0.081	0.940	0.440	75.250	0.888	414.823	6.559	0.276	0.988	34.605	3.546	0.816
Cr-TC (50 mg/L)	499.270	0.066	0.967	0.473	59.776	0.916	378.460	7.701	0.256	0.987	35.904	2.694	0.837
Ni	459.559	0.092	0.982	0.431	69.741	0.923	367.336	4.404	0.337	0.983	33.943	2.409	0.903
Ni-TC (10 mg/L)	422.914	0.087	0.978	0.417	66.063	0.931	338.810	5.395	0.304	0.978	41.130	3.542	0.879
Ni-TC (25 mg/L)	407.673	0.070	0.981	0.434	56.750	0.947	367.336	4.404	0.337	0.983	49.439	5.154	0.833
Ni-TC (50 mg/L)	410.763	0.059	0.975	0.468	47.717	0.938	310.457	9.091	0.235	0.977	41.378	2.074	0.876

mol·K), reflecting substantial disorder because of stronger Pb interactions with the adsorbent.

4. Conclusions

This study investigated tetracycline (TC) and heavy metal (Pb, Cr, and Ni) adsorption and co-adsorption on a magnetic-chitosan-*Arthrospira platensis* (MCA) biocomposite in batch experiments. Results have

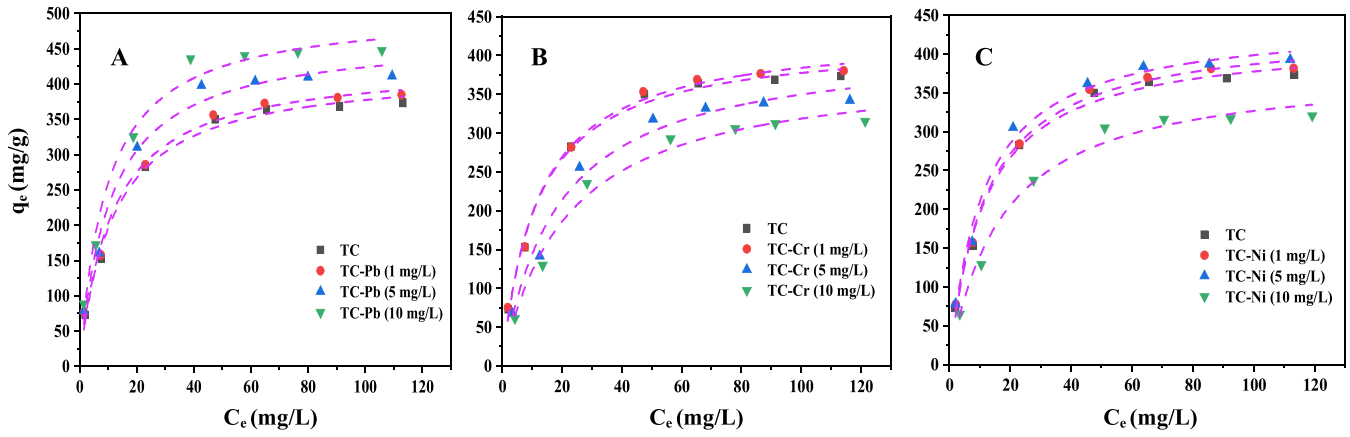

Fig. 6. Langmuir isotherms of TC adsorption in the presence of Pb (A), Cr (B), and Ni (C) at different initial concentrations (5, 10, and 20 mg/L).

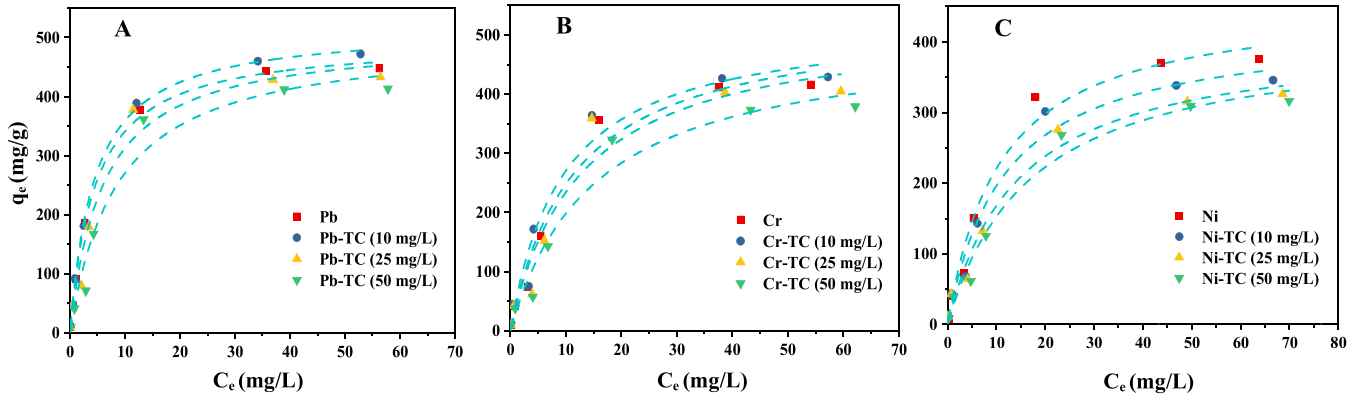

Fig. 7. Langmuir isotherms of Pb (A), Cr (B), and Ni (C) adsorption, in the presence of TC at different concentrations (10, 25, and 50 mg/L).

Table 3
Thermodynamic parameters for adsorption and co-adsorption of TC and heavy metals onto MCA. Parameters: standard changes in Gibbs free energy (ΔG°), enthalpy (ΔH°), and entropy (ΔS°).

Adsorbate	ΔG° (kJ/mol)			ΔH° (kJ/mol)	ΔS° (J/K.mol)
	298 K	308 K	318 K		
TC (50 mg/L)	-6.173	-6.991	-7.810	18.212	81.828
TC-Pb (10 mg/L)	-6.850	-7.493	-8.137	12.342	64.401
TC-Cr (10 mg/L)	-5.218	-5.630	-6.042	7.052	41.176
TC-Ni (10 mg/L)	-5.254	-5.583	-5.912	4.551	32.904
Pb (10 mg/L)	-10.974	-11.909	-12.843	16.882	93.474
Pb-TC (25 mg/L)	-9.019	-9.833	-10.647	15.240	81.405
Cr (10 mg/L)	-7.815	-8.710	-9.607	18.881	89.584
Cr-TC (25 mg/L)	-6.828	-7.501	-8.174	13.218	67.271
Ni (10 mg/L)	-7.723	-8.666	-9.608	20.370	94.272
Ni-TC (25 mg/L)	-7.519	-8.548	-9.576	23.128	102.844

shown how complex the interactions are between TC and heavy metals during their adsorption onto the biocomposite, with the type and concentration of the pollutants affecting both synergistic and competitive interactions. The removal efficiency of TC alone (C_0=50 mg/L) was 54% within 180 min. The co-presence of Pb at lower concentrations (5 and 10 mg/L) was found to enhance TC adsorption through a synergistic bridging effect, whereas Pb at a higher level (20 mg/L) reduced it due to saturation of the active sites. Cr and Ni exhibited competitive adsorption and adversely affected the efficiency of TC removal at higher concentrations. In the same manner, the efficiencies of Pb, Cr, and Ni removal were influenced by the presence of TC. Pb clearly showed very good adsorption capacity in the whole range studied range with the increase in TC concentration. The kinetic study indicated that the pseudo-second-order (PSO) model was able to best describe the adsorption behavior of both TC and heavy metals, thereby suggesting chemisorption governs the adsorption process. Isotherm analysis showed that the Langmuir model provided the most suitable fit, thus confirming monolayer adsorption. Thermodynamic study confirmed that TC and heavy metals adsorption onto the biocomposite was spontaneous and endothermic. These findings have important implications for the optimization of biocomposite-based adsorbents with the aim of simultaneously removing antibiotics and heavy metals from aquatic environments.

CRediT authorship contribution statement

Alessandro Alberto Casazza: Writing – review & editing, Writing – original draft, Supervision, Resources, Methodology, Conceptualization. **Shabnam Mirizadeh:** Writing – review & editing, Writing – original draft, Methodology, Investigation, Formal analysis, Conceptualization. **Attilio Converti:** Writing – review & editing, Writing – original draft, Supervision, Resources.

Declaration of Competing Interest

The authors declare that they have no known competing financial interests or personal relationships that could have appeared to influence the work reported in this paper.

Data availability

Data will be made available on request.

References

[1] Y. Shu, D. Li, T. Xie, K. Zhao, L. Zhou, F. Li, Antibiotics-heavy metals combined pollution in agricultural soils: Sources, fate, risks, and countermeasures, Green. Energy Environ. (2024), https://doi.org/10.1016/j.gee.2024.07.007.

[2] V. Saxena, Water Quality, Air pollution, and climate change: Investigating the environmental impacts of industrialization and urbanization, Water Air Soil Pollut. 236 (2025) 73, https://doi.org/10.1007/s11270-024-07702-4.

[3] S. Akhter, M.A. Bhat, S. Ahmed, W.A. Siddiqui, Antibiotic residue contamination in the aquatic environment, sources and associated potential health risks, Environ. Geochem. Health 46 (2024) 387, https://doi.org/10.1007/s10653-024-02146-5.

[4] S. Ray, R. Vashishth, From water to plate: Reviewing the bioaccumulation of heavy metals in fish and unraveling human health risks in the food chain, Emerg. Contam. 10 (2024) 100358, https://doi.org/10.1016/j.emcon.2024.100358.

[5] L. Xu, H. Zhang, P. Xiong, Q. Zhu, C. Liao, G. Jiang, Occurrence, fate, and risk assessment of typical tetracycline antibiotics in the aquatic environment: A review, Sci. Total Environ. 753 (2021) 141975, https://doi.org/10.1016/j.scitotenv.2020.141975.

[6] J. Antos, M. Piosik, D. Ginter-Kramarczyk, J. Zembrzuska, I. Kruszelnicka, Tetracyclines contamination in European aquatic environments: A comprehensive review of occurrence, fate, and removal techniques, Chemosphere 353 (2024) 141519 https://doi.org/10.1016/j.chemosphere.2024.141519.

[7] A.K. Sarmah, M.T. Meyer, A.B.A. Boxall, A global perspective on the use, sales, exposure pathways, occurrence, fate and effects of veterinary antibiotics (VAs) in the environment, Chemosphere 65 (2006) 725–759, https://doi.org/10.1016/j.chemosphere.2006.03.026.

[8] Z. Wang, Q. Chen, J. Zhang, J. Dong, H. Yan, C. Chen, R. Feng, Characterization and source identification of tetracycline antibiotics in the drinking water sources of the lower Yangtze River, J. Environ. Manag. 244 (2019) 13–22, https://doi.org/10.1016/j.jenvman.2019.04.070.

[9] F. Ahmad, D. Zhu, J. Sun, Environmental fate of tetracycline antibiotics: degradation pathway mechanisms, challenges, and perspectives, Environ. Sci. Eur. 33 (2021) 64, https://doi.org/10.1186/s12302-021-00505-y.

[10] W. Xu, Y. Jin, G. Zeng, Introduction of heavy metals contamination in the water and soil: a review on source, toxicity and remediation methods, Green. Chem. Lett. Rev. 17 (2024) 2404235, https://doi.org/10.1080/17518253.2024.2404235.

[11] M. Moghimi Dehkordi, Z. Pournuroz Nodeh, K. Soleimani Dehkordi, H. salmanvandi, R. Rasouli Khorjestan, M. Ghaffarzadeh, Soil, air, and water pollution from mining and industrial activities: Sources of pollution, environmental impacts, and prevention and control methods, Results Eng. 23 (2024) 102729, https://doi.org/10.1016/j.rineng.2024.102729.

[12] E. Kravchenko, T. Minkina, S. Mandzhieva, T. Bauer, E. Lacynnik, M.H. Wong, O. Nazarenko, Ecological and health risk assessments of heavy metal contamination in soils surrounding a coal power plant, J. Hazard. Mater. 484 (2025) 136751, https://doi.org/10.1016/j.jhazmat.2024.136751.

[13] P.B. Angon, M.S. Islam, S. KC, A. Das, N. Anjum, A. Poudel, S.A. Suchi, Sources, effects and present perspectives of heavy metals contamination: Soil, plants and human food chain, Heliyon 10 (2024), https://doi.org/10.1016/j.heliyon.2024.e28357.

[14] C. Li, F. Luo, H. Duan, F. Dong, X. Chen, M. Feng, Z. Zhang, L. Cizmas, V.K. Sharma, Degradation of chloramphenicol by chlorine and chlorine dioxide in a pilot-scale water distribution system, Sep. Purif. Technol. 211 (2019) 564–570, https://doi.org/10.1016/j.seppur.2018.10.019.

[15] S. Li, Y. Wu, H. Zheng, H. Li, Y. Zheng, J. Nan, J. Ma, D. Nagarajan, J.-S. Chang, Antibiotics degradation by advanced oxidation process (AOPs): Recent advances in ecotoxicity and antibiotic-resistance genes induction of degradation products, Chemosphere 311 (2023) 136977, https://doi.org/10.1016/j.chemosphere.2022.136977.

[16] J.S. Sravan, L. Matsakas, O. Sarkar, Advances in biological wastewater treatment processes: focus on low-carbon energy and resource recovery in biorefinery context, Bioengineering 11 (2024), https://doi.org/10.3390/bioengineering11030281.

[17] A. Moghaddam, D. Khayatan, P. Esmaeili Fard Barzegar, R. Ranjbar, M. Yazdanian, E. Tahmasebi, M. Alam, K. Abbasi, H. Esmaeili Gouvarchin Ghaleh, H. Tebyaniyan, Biodegradation of pharmaceutical compounds in industrial wastewater using biological treatment: a comprehensive overview, Int. J. Environ. Sci. Technol. 20 (2023) 5659–5696, https://doi.org/10.1007/s13762-023-04880-2.

[18] P.R. Rout, T.C. Zhang, P. Bhunia, R.Y. Surampalli, Treatment technologies for emerging contaminants in wastewater treatment plants: A review, Sci. Total Environ. 753 (2021) 141990, https://doi.org/10.1016/j.scitotenv.2020.141990.

[19] S. Satyam, S. Patra, Innovations and challenges in adsorption-based wastewater remediation: A comprehensive review, Heliyon 10 (2024) e29573, https://doi.org/10.1016/j.heliyon.2024.e29573.

[20] Y. Zohrabi, Synthesis and application of magnetic ferrites (MFe2O4) in the removal of heavy metals from aqueous solutions: An updated review, Mater. Sci. Eng. B. 299 (2024) 117024, https://doi.org/10.1016/j.mseb.2023.117024.

[21] A. Balakrishnan, S. Appunni, M. Chinthala, M.M. Jacob, D.-V.N. Vo, S.S. Reddy, E. S. Kunnel, Chitosan-based beads as sustainable adsorbents for wastewater remediation: a review, Environ. Chem. Lett. (2023), https://doi.org/10.1007/s10311-023-01563-9.

[22] I. Olalekan, W. Da, F. Bukhari, M. Suah, Chitosan modifications for adsorption of pollutants – A review, J. Hazard. Mater. 408 (2021) 124889, https://doi.org/10.1016/j.jhazmat.2020.124889.

[23] S. Sun, H. Zeng, H. Xu, W. Zhao, W. Qi, R. Hao, J. Zhang, D. Li, Adsorption of As(V) and P(V) by magnetic iron-based alginate-chitosan beads: Competitive adsorption and reduction mechanism of As(V) induced by Fe(II), Colloids Surf. A Physicochem. Eng. Asp. 675 (2023) 132068, https://doi.org/10.1016/j.colsurfa.2023.132068.

[24] S. Mirizadeh, A. Converti, A.A. Casazza, Chitosan-based adsorbents for antibiotic removal with insights from batch and dynamic studies: A review, Int. J. Biol. Macromol. 331 (2025) 148399, https://doi.org/10.1016/j.ijbiomac.2025.148399.

[25] D.A. Gkika, A.C. Mitropoulos, P. Kokkinos, D.A. Lambropoulou, I.K. Kalavrouziotis, D.N. Bikiaris, G.Z. Kyzas, Modified chitosan adsorbents in pharmaceutical simulated wastewaters: A review of the last updates, Carbohydr. Polym. Technol. Appl. 5 (2023) 100313, https://doi.org/10.1016/j.carpta.2023.100313.

[26] Y. Li, H. Zhang, G. Qu, L. Xie, S. Tang, H. Lei, Y. Zhong, Y.-F. Zhang, Efficient removal of antibiotics from wastewater by chitosan/polyethyleneimine/Ti3C2 MXene composite hydrogels: Synthesis, adsorption, kinetics and mechanisms, Colloids Surf. A Physicochem. Eng. Asp. 702 (2024) 135111, https://doi.org/10.1016/j.colsurfa.2024.135111.

[27] X. Jia, Y. Huang, J. Zhu, S.A. Junejo, B. Zhang, Q. Huang, Fabrication of genipin cross-linked chitosan-ZIF-8 through emulsion templated approach for sulfanilamide removal, Mater. Sci. Eng. B. 313 (2025) 117933, https://doi.org/10.1016/j.mseb.2024.117933.

[28] S. Mirizadeh, A.A. Casazza, A. Converti, Removal of tetracycline and crystal violet from aqueous solutions by magnetic chitosan-lipid free *Chlorella vulgaris* biocomposite, Sep. Purif. Technol. 368 (2025) 132919, https://doi.org/10.1016/j.seppur.2025.132919.

[29] L. Zhang, L. Yang, F. Yi, Y. Yang, X. You, M. Yang, Y. Hong, J. Chen, Y. Zhang, X. Zhou, Experimental and theoretical study of multiple active site-functionalized Spirulina residue-based porous carbon as an economical adsorbent for NH3 and SO2 adsorption: Micro- and macro-mechanistic investigations, J. Clean. Prod. 469 (2024), https://doi.org/10.1016/j.jclepro.2024.143167.

[30] M.B. Yahia, R. Gerhardt, L. Sellaoui, H.Y.S. Al-Zahrani, A.P.O. Inácio, D. Dias, T.R. S. Cadaval, L.A. de Almeida Pinto, A. Bonilla-Petriciolet, M. Badawi, An emerging application of chitosan and chitosan/*spirulina* films for Pb2+ adsorption: New physicochemical insights via experimental and theoretical studies, Sep. Purif. Technol. 337 (2024), https://doi.org/10.1016/j.seppur.2024.126451.

[31] X. Sun, H. Huang, Y. Zhu, Y. Du, L. Yao, X. Jiang, P. Gao, Adsorption of Pb2+ and Cd2+ onto *Spirulina platensis* harvested by polyacrylamide in single and binary solution systems, Colloids Surf. A Physicochem. Eng. Asp. 583 (2019) 123926, https://doi.org/10.1016/j.colsurfa.2019.123926.

[32] S. Mirizadeh, C. Solisio, A. Converti, A.A. Casazza, Efficient removal of tetracycline, ciprofloxacin, and amoxicillin by novel magnetic chitosan/microalgae biocomposites, Sep. Purif. Technol. (2023) 125115, https://doi.org/10.1016/j.seppur.2023.125115.

[33] A. Yadav, N. Bagotia, A.K. Sharma, S. Kumar, Simultaneous adsorptive removal of conventional and emerging contaminants in multi-component systems for wastewater remediation: A critical review, Sci. Total Environ. 799 (2021) 149500, https://doi.org/10.1016/j.scitotenv.2021.149500.

[34] J. Bayuo, M.J. Rwiza, M. Sillanpää, K.M. Mtei, Removal of heavy metals from binary and multicomponent adsorption systems using various adsorbents – a systematic review, RSC Adv. 13 (2023) 13052–13093, https://doi.org/10.1039/D3RA01660A.

[35] F. Tong, D. Liu, Z. Zhang, W. Chen, G. Fan, Y. Gao, X. Gu, C. Gu, Heavy metal-mediated adsorption of antibiotic tetracycline and ciprofloxacin on two microplastics: Insights into the role of complexation, Environ. Res. 216 (2023) 114716, https://doi.org/10.1016/j.envres.2022.114716.

[36] H. Jiao, M. Cui, S. Yuan, B. Dong, Z. Xu, Carbon nanomaterials for co-removal of antibiotics and heavy metals from water systems: An overview, J. Hazard. Mater. 489 (2025) 137566, https://doi.org/10.1016/j.jhazmat.2025.137566.

[37] Y. Zhao, Y. Tan, Y. Guo, X. Gu, X. Wang, Y. Zhang, Interactions of tetracycline with Cd (II), Cu (II) and Pb (II) and their cosorption behavior in soils, Environ. Pollut. 180 (2013) 206–213, https://doi.org/10.1016/j.envpol.2013.05.043.

[38] R. Pulicharla, K. Hegde, S.K. Brar, R.Y. Surampalli, Tetracyclines metal complexation: Significance and fate of mutual existence in the environment, Environ. Pollut. 221 (2017) 1–14, https://doi.org/10.1016/j.envpol.2016.12.017.

[39] L. Lin, S. Tang, X. Sun, A. Feng, W. Liang, X. Wang, Adsorption of Pb(II) ions and tetracycline onto microplastics: Interaction mechanisms and synergistic effects, Huanjing Kexue Xuebao/Acta Sci. Circumstantiae 41 (2021) 4022–4031, https://doi.org/10.13671/j.hjkxxb.2021.0052.

[40] L. Zhou, X. Zhu, T. Chi, B. Liu, C. Du, G. Yu, H. Wu, H. Chen, Reutilization of manganese enriched biochar derived from *Phytolacca acinosa* Roxb. residue after phytoremediation for lead and tetracycline removal, Bioresour. Technol. 345 (2022), https://doi.org/10.1016/j.biortech.2021.126546.

[41] L. Jing, W. Xuejiang, W. Yuan, X. Siqing, Z. Jianfu, Insight into the co-adsorption behaviors and interface interactions mechanism of chlortetracycline and lead onto struvite loaded diatomite, J. Hazard. Mater. 405 (2021) 124210, https://doi.org/10.1016/j.jhazmat.2020.124210.

[42] X. Zheng, C. Pan, S. Zheng, Y. Guo, Functionalized magnetic chitosan-based adsorbent for efficient tetracycline removal: Deep investigation of adsorption behaviors and mechanisms, Sep. Purif. Technol. 335 (2024), https://doi.org/10.1016/j.seppur.2023.126212.

[43] T.M.H. Tran, T.D. Tran, T.D. Dinh, M.K. Nguyen, N.T.N. Anh, N.K. Nga, T.H. Y. Doan, T.D. Pham, Adsorption characteristics of individual and binary mixtures

of ciprofloxacin and Cr(VI) in water using MnO2 colloidal particles, Colloid Polym. Sci. 302 (2024) 1395–1405, https://doi.org/10.1007/s00396-024-05275-6.
[44] Z. Zhou, Y. Sun, Y. Wang, F. Yu, J. Ma, Adsorption behavior of Cu(II) and Cr(VI) on aged microplastics in antibiotics-heavy metals coexisting system, Chemosphere 291 (2022) 132794, https://doi.org/10.1016/j.chemosphere.2021.132794.
[45] S. Guo, W. Zhang, Y. Liu, S. Tan, H. Cai, J. Geng, X. Liu, Effective removal of Pb(II) from multiple cationic heavy metals—An inexpensive lignin-modified attapulgite, Sustainability 16 (2024), https://doi.org/10.3390/su16145831.
[46] M.G. Genduso, M. Guagliano, E. Finocchio, C. Cristiani, G. Dotelli, G. Santomauro, Adsorption of heavy metals from low concentration solutions onto dried *Chlamydomonas reinhardtii*, Appl. Sci. 14 (2024), https://doi.org/10.3390/app142311057.
[47] Y. Sun, Q. Yue, B. Gao, Y. Gao, X. Xu, Q. Li, Y. Wang, Adsorption and cosorption of ciprofloxacin and Ni(II) on activated carbon-mechanism study, J. Taiwan Inst. Chem. Eng. 45 (2014) 681–688, https://doi.org/10.1016/j.jtice.2013.05.013.
[48] J. Deng, X. Li, X. Wei, Y. Liu, J. Liang, B. Song, Y. Shao, W. Huang, Hybrid silicate-hydrochar composite for highly efficient removal of heavy metal and antibiotics: Coadsorption and mechanism, Chem. Eng. J. 387 (2020) 124097, https://doi.org/10.1016/j.cej.2020.124097.
[49] D. Balarak, F. Mostafapour, A. Joghtaei, Thermodynamic analysis for adsorption of amoxicillin onto magnetic carbon nanotubes, Br. J. Pharm. Res. 16 (2017) 1–11, https://doi.org/10.9734/bjpr/2017/33212.
[50] A. Fathollahi, S.J. Coupe, A.H. El-Sheikh, L.A. Sañudo-Fontaneda, The biosorption of mercury by permeable pavement biofilms in stormwater attenuation, Sci. Total Environ. 741 (2020) 140411, https://doi.org/10.1016/j.scitotenv.2020.140411.
[51] Y. Wang, C. Wang, X. Huang, Q. Zhang, T. Wang, X. Guo, Guideline for modeling solid-liquid adsorption: Kinetics, isotherm, fixed bed, and thermodynamics, Chemosphere 349 (2024) 140736 ttps://doi.org/10.1016/j.chemosphere.2023.140736.